

Kinematics of Polymer Chains in Dense Medium. 4. Effect of Backbone Geometry and Application to Polybutadiene

C. Baysal, I. Bahar,* and B. Erman

Polymer Research Center, School of Engineering, Bogazici University, and TUBITAK Advanced Polymeric Materials Research Center, Bebek 80815, Istanbul, Turkey

L. Monnerie

Ecole Supérieure de Physique et Chimie Industrielle, PCSM, 10 Rue Vauquelin, Cedex 05, Paris 75231, France

Received June 16, 1995; Revised Manuscript Received December 6, 1995[⊗]

ABSTRACT: The present study is an extension of the *cooperative kinematics* (CK) approach (Bahar, I.; Erman, B.; Monnerie, L. *Macromolecules* **1992**, *25*, 6309), which has been demonstrated to give an efficient and realistic account of the mechanism of local relaxational processes in polyethylene (PE). In the present work, the effects of (i) departure from tetrahedral backbone geometry and (ii) differences in torsional potentials of backbone bonds are addressed by considering *cis*- and *trans*-polybutadiene (PBD) chains. The method is based on the minimization of the atomic displacements of chain units and the torsional energy changes, succeeding the isomerization of a given bond. In contrast to the highly localized response of PE to bond rotational jumps, in which the strongest coupling between rotational motions was observed between second neighboring bonds, the coupling in PBD is shown to involve longer chain segments, embodying the strongly correlated torsions of third or fourth neighboring bonds along the chain. The mechanism of motion is unique for each type of rotating bond for *cis* and *trans* structures: In *trans*-PBD, strong counterrotations are encountered at the second neighboring bonds separated by a double bond, whereas in *cis*-PBD, the same pair of bonds undergoes coupled corotations. Orientational and translational motions of chain units located between successive double bonds are significantly affected by nonbonded intramolecular interactions in *cis*-PBD, while this effect is not seen in the *trans* structure. Changes in environmental conditions do not affect the mechanism of localization phenomena, but rather modulate the amplitudes of motion. Under the same frictional environment, *cis*-PBD atomic displacements are larger than those in *trans*-PBD by a factor of ~ 1.5 . The predictions of the theory are in good agreement with the results from recent molecular dynamics (MD) simulations of PBD (Kim, E.-G.; Mattice, W. L. *J. Chem. Phys.* **1994**, *101*, 6242; Gee, R. H.; Boyd, R. H. *J. Chem. Phys.* **1994**, *101*, 8028). More interestingly, good agreement between the results obtained for *cis*-PBD and those from the bulk state MD simulations of *cis*-polyisoprene (Moe, N. E.; Ediger, M. D. *Polymer*, submitted) is found, confirming that backbone geometry has the major role in determining the mechanism of local conformational relaxations. An advantage of the present approach is that the computational time required is at least 2 orders of magnitude less than that of conventional MD simulations.

Introduction

The problem of cooperativity between the motions of chain units in polymers during the rotameric transition of a given bond is central to the study of local polymer dynamics. From spectroscopic measurements and numeric simulations, it is now known that the motions induced by rotameric jumps are highly localized in space for chains in the bulk state as well as for those in dilute solution.^{1–6} The localization is established through correlations between the motion of the bond undergoing the rotameric transition and the neighboring atoms, either along the chain or in the surrounding medium.

The kinetic theory of conformational transitions in polymers was first developed by Helfand.¹ Later, the problem was explored by using computational methods such as Brownian dynamics (BD)^{4,5,7–9} and molecular dynamics (MD) simulations.^{10–15} Although these techniques were initially utilized on the simplest model chains of polyethylene (PE) in solution, they were later applied to other synthetic polymers both in solution and in bulk. On the other hand, approaches based on master equation formalism^{16–19} were also developed; among them the dynamic rotational isomeric state

(DRIS) model²⁰ adopted real chain conformational and structural characteristics. The state of the art on the utilization of computer methods for investigating chain dynamics is reviewed by Ediger and Adolf⁵ and by Bahar *et al.*⁶

In a recent series of papers,^{21–23} the correlated motions of chain atoms in dense medium are investigated. In these studies, the term dense medium is used with reference to polymers in the bulk state above the glass transition temperature, where the femtosecond librations and fluctuations due to acceleration are neglected. The most probable trajectory of chain atoms accompanying the rotameric transitions of a given bond from one rotational isomeric minimum to another is obtained by considering the torsional potentials and the frictional resistance exerted by the environment.²³ Calculations using this scheme, termed *cooperative kinematics* (CK), show that the mechanism of localization involves three types of motions of neighboring bonds. (i) Correlated torsions: For PE, a rotational transition results in correlated torsions up to sixth neighboring bonds on each side of the rotating bond. The second neighbors show the strongest response in the form of a counterrotation. (ii) An overall reorientation, in space, of a few bonds, including and adjoining the bond that undergoes the rotameric transition: In PE, the bond undergoing

[⊗] Abstract published in *Advance ACS Abstracts*, February 15, 1996.

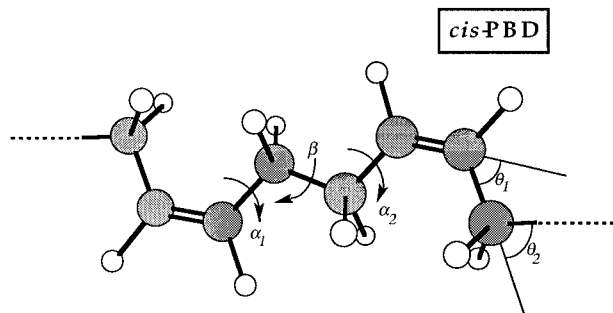


Figure 1. Segment of *cis*-PBD chain. Three types of backbone bonds exist in each repeat unit: a double bond connecting two sp^2 carbon atoms, a β bond connecting two sp^3 carbon atoms, and α_1 and α_2 bonds connecting sp^2 and sp^3 carbon atoms. α_1 and α_2 are identical in PBD and are generally referred to as α bonds in the text. Supplements of the two distinct types of bond angles, θ_1 and θ_2 , are also displayed.

the rotameric transition is itself reoriented by about 25–35°. The first neighbors on each side exhibit the largest reorientations (~50–60°), and the extent of reorientation is vanishingly small beyond sixth neighbors. (iii) Displacement of atoms in space: For PE, mean translations of about 0.8 Å were observed in the atoms located at both ends of the rotating bond. These results, which are obtainable with a minimum computational effort by the CK approach, were shown to conform closely with those extracted from BD runs.

BD and MD simulations carried out for different polymers, and in particular the comparison of the results for PE and polyisoprene (PIP),²⁴ suggest that the local chain geometry is an important property determining the type and strength of intramolecular correlations. In the present paper, we investigate the kinematics of polybutadiene (PBD) chains in dense environments to assess the possible importance of chain geometry. Due to the presence of double bonds and nontetrahedral bond angles along the backbone, as well as the possibility of *cis* and *trans* isomers, the backbone geometry of these chains significantly departs from that of PE studied in refs 21–23.

In the following section, the model and the basic assumptions of the approach are briefly described. The results for PBD are compared with recent MD simulations of PBD^{14,15} and polyisoprene²⁵ in the bulk state. The predominant role of the backbone geometry in prescribing the mechanism of local conformational motions is emphasized. In the final section, a few concluding remarks are presented and possible future applications of CK are discussed.

Model and Assumptions

Chain Model. A segment of a *cis*-PBD chain of n backbone bonds is presented in Figure 1. The backbone carbon atoms and their pendant hydrogens are taken as united groups. All bond lengths, l , and bond angles, θ , are fixed to their equilibrium values. Only the dihedral angles, φ_i , about the single bonds are assumed to rotate. The bonds labeled α_1 and α_2 in the figure are structurally equivalent and will be referred to as α bonds throughout the text. The rotatable $\text{CH}_2\text{--CH}_2$ bond confined between two α bonds is termed as the β type. The structure shown in Figure 1 corresponds to the *cis* isomer. The *trans* isomer is obtained by a 180° rotation about the double bonds. Thus, a repeat unit comprises one double bond, one bond of type β , and two bonds of type α .

Table 1. Torsional Potential Parameters

	α bond	β bond	double bond
k_φ (J/mol)	2594.3	8088.7	2.60×10^6
a_0	1.00	1.00	1.00
a_1	6.27	1.92	$\pm 2.00^a$
a_2	0.18	-0.55	1.00
a_3	7.45	-1.91	0.00
a_4	0.00	1.10	0.00
a_5	0.00	-1.56	0.00

^a +2.00 for *cis*-PBD and -2.00 for *trans*-PBD.

The rotational potential of each backbone bond is expressed as a polynomial of the form

$$V_{\varphi_i} = k_\varphi \sum_{m=0}^5 a_m \cos^m \varphi_i \quad (1)$$

The values of k_φ and the coefficients a_m are taken from ref 26. These are given in Table 1 according to the type of bond considered. An average value of 1.5 Å is adopted for all bond lengths for computational simplicity, although we note that the double bond is shorter (~1.32 Å), the α bond is 1.53 Å, and the β bond is 1.51 Å. The supplements of the bond angles defined by $\text{CH--CH}_2\text{--CH}_2$ and CH--CH--CH_2 units are fixed at the respective values of $\theta_1 = 65.4^\circ$ and $\theta_2 = 60.0^\circ$.

Basic Approach. The Lagrange equation of motion for a chain is expressed as

$$\frac{d}{dt} \left[\frac{\partial L}{\partial \dot{q}_j} \right] - \frac{\partial L}{\partial q_j} + \frac{\partial F}{\partial q_j} = 0 \quad (2)$$

where \mathbf{q} represents the set of generalized coordinates, the dot denotes the time derivative, L is the Lagrangian, and F is Rayleigh's dissipation function, whose gradient with respect to the velocity of any atom gives the frictional force experienced by that atom. Backbone atoms are numbered from 0 to $n+1$. The set \mathbf{q} includes the following variables: (i) the position vector $\mathbf{R}_0 = \text{col}[X_0, Y_0, Z_0]$ of the zeroth atom relative to a laboratory-fixed coordinate system, (ii) the Euler angles, Φ , Ψ , and χ , defining the absolute orientation of the chain in space, and (iii) the internal torsional angles, φ_i . In a highly viscous medium, such as that experienced by a polymer chain in the bulk state, the kinetic energy term in L and the acceleration contribution may be neglected, and the equation of motion simplifies to

$$\frac{\partial V}{\partial q_j} + \frac{\partial F}{\partial \dot{q}_j} = 0 \quad (3)$$

where V is the potential. Following this approximation, the problem of finding the optimal changes in the generalized coordinates in response to a torsional rotation reduces to the solution of

$$\frac{\partial V}{\partial \varphi_i} + \frac{1}{2} \frac{\partial \delta W_\xi}{\partial \delta \varphi_i} = 0; \quad 2 \leq i \leq (n-1) \quad (4)$$

$$\frac{\partial \delta W_\xi}{\partial \delta \Phi} = \frac{\partial \delta W_\xi}{\partial \delta \Psi} = \frac{\partial \delta W_\xi}{\partial \delta \chi} = \frac{\partial \delta W_\xi}{\partial \delta \mathbf{R}_0} = 0$$

Here δW_ξ denotes the differential work done by the chain against friction during small incremental displacements $\delta \mathbf{R}_i$ in chain units occurring within short time intervals δt . It is expressed in terms of the Rayleigh dissipation function and the effective friction coefficient ξ as

$$\delta W_{\xi} = 2F\delta t = (\xi/\delta t) \sum_i \delta \mathbf{R}_i \cdot \delta \mathbf{R}_i \quad (5)$$

For a complete derivation of the preceding equations and a detailed presentation of the mathematical formalism of the CK approach, the reader is referred to our previous work.²³

Results of Calculations and Discussion

General Calculation Procedure. According to the CK approach, either an α or a β bond in the middle of the chain is rotated by small increments, and the new values of the other degrees of freedom are determined at each step from the simultaneous solution of the $n + 4$ equations implicit in eq 4. The incremental variation procedure is repeated until the rotating bond completes a full isomeric transition. This operation leads to the cooperative response of all of the chain elements in the particular original configuration to the rotational isomerization of the given bond. The mathematical details of the minimization procedure may be found elsewhere.²³ For assessing the general response of a chain irrespective of the original configuration, it is essential to take the average over an ensemble of chains. A total of 500 such Monte Carlo (MC) chains is generated for the cases of *all-cis*- or *all-trans*-PBD, although averaging over 50 chains has been verified to yield approximately the same results. In MC generations, dihedral bond angles are assigned to each bond in conformity with their equilibrium distribution of rotational states in PBD repeat units. The states accessible to different types of bonds and their probabilities are presented in Table 2.^{27–29} In *trans*-PBD, there is a third-order interdependence between the α_1 and α_2 bonds located within a repeat unit.²⁷ The conditional probabilities calculated from the statistical weight matrices provided in ref 27 are presented in Table 3. It is shown in the table that the conditional probabilities are rather close to those of the independent bonds presented in Table 2. In fact, our calculations show that results obtained by using conditional probabilities differ insignificantly from those obtained by the use of independent probabilities.

Calculations are performed for $n = 25$. No major differences are observed between the results for $n = 25$ and 39 bonds, as in the previous study,²³ which confirms that the motion is localized to only a few neighboring units.

In the previous study, results were conveniently expressed in terms of a dimensionless ratio relating the strength of the two factors affecting the mechanism of motion, i.e., the frictional resistance and the internal rotational barriers:²³

$$k_0 = \frac{2k_{\varphi}}{f\xi/\Delta t} \quad (6)$$

Here Δt is the mean isomerization time of dihedral angles. In this study, the k_0 value must be selected carefully because there are three different types of bonds on the backbone, and the rotational potential coefficient k_{φ} takes on distinct values depending on the bond considered (Table 1). To be able to compare the results obtained for PE and PBD in the same frictional environment, it proves convenient to fix k_{φ} of the β bond (8.09 kJ/mol) for all classes of bonds and rescale the a_m values.

In the following, *cis*- and *trans*-PBD are considered separately and their mechanisms of localization of

Table 2. Rotational Isomeric States of Each Type of Bond in PBD and Their Equilibrium Probabilities

bond type	isomeric states ^a and their probabilities ^b		
	A^+	A^-	t
α bond (<i>cis</i> -PBD)	A^+ (0.48)	A^- (0.48)	t (0.04)
α bond (<i>trans</i> -PBD)	A^+ (0.44)	A^- (0.44)	c (0.12)
β bond	t (0.38)	g^+ (0.31)	g^- (0.31)
double bond ^c	t/c (1.00)		

^a t , *trans* (0°); c , *cis* (180°); A^\pm , anticlinal ($\pm 60^\circ$); g^\pm : *gauche* ($\pm 120^\circ$). ^b In parentheses. ^c Depends on *cis* and *trans* forms.

Table 3. Conditional Probabilities for *trans*-PBD Bonds in a Repeat Unit

state of $\alpha_1\beta$	state of α_2		
	c	A^+	A^-
ct	0.12	0.44	0.44
A^+t	0.12	0.44	0.44
A^-t	0.12	0.44	0.44
cg^+	0.12	0.44	0.44
A^+g^+	0.02	0.49	0.49
A^-g^+	0.02	0.49	0.49
cg^-	0.12	0.44	0.44
A^+g^-	0.02	0.49	0.49
A^-g^-	0.02	0.49	0.49

motion in various environmental conditions are compared. The response to 120° rotation of each type of bond, α and β , in the middle of the chain is considered for both stereoisomers. In each case, the kinematics is analyzed from three perspectives: (i) changes in dihedral angles, (ii) angular displacement of backbone bonds, and (iii) translation of chain atoms.

β Bond Isomerization. The β bond is composed of two tetrahedrally bonded CH_2 groups; this type of bond is common to PE and PBD and therefore allows for the comparison of the behavior of PE, *cis*-PBD, and *trans*-PBD chain segments, in response to the isomerization of the given type of bond. The localization mechanism for each of the three polymers is investigated for $k_0l^2 = 0.01 \text{ \AA}^2$ or $\xi/\Delta t = 1.62 \times 10^8 \text{ kg/(mol}\cdot\text{ns}^2)$, which is approximately representative of the frictional resistance experienced by flexible chains in a dense environment, as previously discussed.²³ The torsional motions of the neighboring bonds accompanying the isomerization of the β bond are presented in Figure 2a,b. In Figure 2a, the change in absolute dihedral angles $\langle |\Delta\varphi_i| \rangle$, averaged over 500 different configurations, is plotted as a function of the serial bond index. The bond undergoing the torsional rotation is shown as the zeroth bond. For both *cis*- and *trans*-PBD, the response of the first neighbors, α bonds, is observed to be stronger than that of farther neighbors. This is different from the behavior of PE, where the tendency of second neighbors to rotate is stronger. Also, in PE, the response of bonds beyond second neighbors is quickly lost, while in PBD the torsional motion of the third and fourth neighbors is quite significant. That of the second neighbor, which is a double bond, is severely restricted.

In Figure 2b, the actual values of torsional rearrangements resulting from the rotational transition of the zeroth bond are presented as a function of bond index. The full 120° rotation of the zeroth bond is not shown along the ordinate to see the rotations of the neighbors on a larger scale. The term *corotation* will be used in the following in reference to torsional motions of bonds in the same sense as the zeroth bond, and *counterrotation* will be used for those in the opposite sense. In PBD, the four nearest neighbors on both sides of the rotating β bond exhibit counterrotations of various amplitudes, whereas in PE the counterrotations are

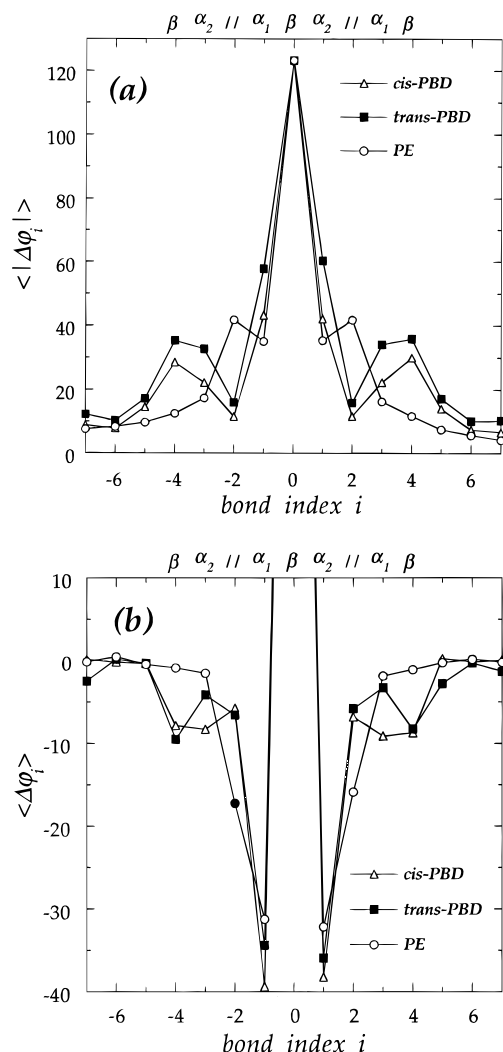


Figure 2. (a) Average absolute changes in dihedral angles, $\langle |\Delta\varphi_i| \rangle$, in response to 120° rotation of β bonds in *cis*- and *trans*-PBD compared with the PE results, with $\xi/\Delta t = 1.62 \times 10^8$ kg/(mol \cdot ns 2). Averaging is performed by solving the set of eq 4 for 500 chain configurations in each case. The rotating bond labeled as the zeroth is in the middle of 25 bond chains. Indexing is performed according to separation from this bond. The identities of the rotated bond and the four bonds on either side are indicated at the top of the figure. The symbol (\parallel) stands for the double bond. (b) Average changes in the dihedral angles of bonds, $\langle \Delta\varphi_i \rangle$, in response to the rotation of β bonds in PE and in *cis*- and *trans*-PBD chains subject to the same conditions as the chains in part a.

confined to the first and second neighbors only. The first neighbor exhibits the largest counterrotation ($\sim 35^\circ$) in all cases. The fourth neighbor, i.e., the β bond of the adjacent repeat unit, is the bond that exhibits the next strongest response in *trans*-PBD, whereas in *cis*-PBD, the counterrotations of the third and fourth neighbors are of comparable strength. Figure 2a,b already reveals that the coupling between bond rotational motions is not confined to nearest neighbors in PBD, but extends to third or fourth neighbors, departing from the behavior of PE bonds.

The spatial reorientations of backbone bonds accompanying the isomerization of the zeroth bond are presented in Figure 3. These angular displacements, including that of the bond undergoing the torsional transition, are postulated to play an important role in localizing the transition.²³ The zeroth bond is observed to reorient by 40–45° in PBD, which is slightly larger

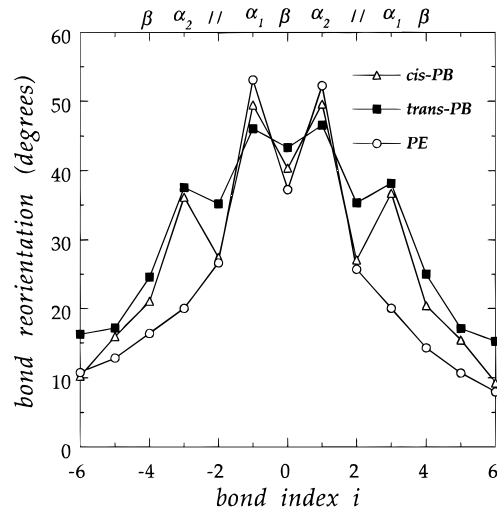


Figure 3. Average spatial reorientations of bond vectors in response to the rotation of β bonds in PE and in *cis*- and *trans*-PBD chains subject to the same environmental conditions as the chains in Figure 2. The rotating bond is in the middle of 25 bond chains and is labeled as the zeroth. Indexing is performed according to separation from this bond. The identities of the rotated bond and the four bonds on either side are indicated at the top of the figure.

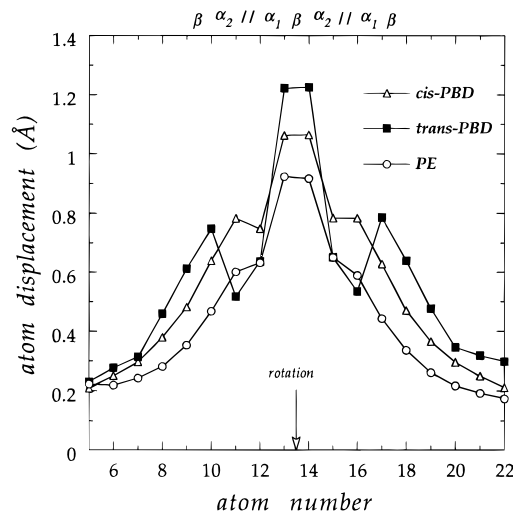


Figure 4. Average spatial displacements of atoms in response to the rotation of β bonds in PE and in *cis*- and *trans*-PBD chains subject to the same environmental conditions as the chains in Figure 2. The bond in the middle of 25 bond chains, connecting atoms 13 and 14, is rotated by 120° as indicated in the figure. The types of the nine bonds in the middle of the chains are given at the top of the figure.

than in PE. The spatial reorientations of the first neighbors for the *trans*- and *cis*-PBD are observed to be 50° , approximately, indicating that the angular change of 109.5° induced by the rotameric jump of the β bond is distributed equally among the first neighboring bonds on both sides. Interestingly, the α bond of the adjoining repeat unit, i.e., the third neighboring bond along the chain, exhibits a large amplitude spatial reorientation in PBD, and in *cis*-PBD in particular, which strongly departs from the behavior of PE.

The average translations of backbone atoms during the rotational isomerization of a central bond are presented in Figure 4. The ordinate represents the mean displacement of the backbone atoms while the β bond between the 13th and 14th atoms undergoes a rotameric transition, as indicated in the figure. The atoms directly attached to the rotating β bond go

through the largest displacement, as expected: 1.2 Å for *trans*-, and 1.0 Å for *cis*-PBD. In *cis*-PBD, the next highest displacement (~ 0.8 Å) is observed in the 11th and 12th atoms and their symmetric counterparts, the 15th and 16th atoms. These are the atoms flanking the two closest neighboring double bonds of the rotating β bond. In *trans*-PBD, on the other hand, the largest displacement (~ 0.8 Å) among neighbors is observed in the 10th atom and its symmetric counterpart, i.e., the 17th. These are the atoms at the inner termini of the nearest β bonds along the chain.

α Bond Isomerization. We note from Table I that the torsional energy barrier associated with α bonds is significantly lower than that of β bonds, which implies that the rotational isomerization of α bonds is more frequent than that of β bonds. This property is also verified by the bulk simulations of Gee and Boyd.¹⁴ The chain response is now asymmetric with respect to the rotating bond. The results are displayed for the rotation of α_1 . The results for α_2 are symmetrically related and are not shown separately.

For comparative purposes, it is more convenient to examine the results obtained under the same frictional environmental resistance as in the previous section. This necessitates the readjustment of k_0 such that the ratio $\xi/\Delta t$ is held constant in analyzing either the α or β bonds. Thus, we introduce the variable $k_0^* \equiv k_0 (k_{\varphi,\beta}/k_{\varphi,\alpha})$, where $k_{\varphi,\alpha}$ and $k_{\varphi,\beta}$ represent the torsional potential barrier heights for α and β bonds, respectively.

The absolute changes in the dihedral angles of *cis*- and *trans*-PBD bonds following the rotation of an α_1 bond, $\langle |\Delta\varphi_i| \rangle$, are presented as solid curves in Figure 5a for $k_0^* \tau^2 = 0.01$ Å² or $\xi/\Delta t = 1.62 \times 10^8$ kg/(mol·ns²). The dashed line is obtained for *cis*-PBD on the basis of a subset of conformations in which the excluded volume effect is taken into consideration; precisely, configurations involving nonbonded atom pairs ($j - i \geq 5$) closer than 3.8 Å are not included in the original set of MC chains. In intermediate or final steps, on the other hand, states violating the excluded volume are verified to be rare and have been neglected. The excluded volume effect is negligibly small in the *trans*-PBD chains of $n = 25$ presently explored.

In both *cis*- and *trans*-PBD, the response of the second neighbors (bond α_2) is found to be quite strong. In *cis*-PBD, the α_2 bond across the β bond exhibits the strongest response, whereas in *trans*-PBD, the nearest α_2 bond across the double bond is rotated by $|\Delta\varphi| > 80^\circ$, on average. The responses of the adjacent β bond ($i = 1$) and the α_2 bond across the β bond ($i = 2$) in *cis*-PBD are significantly affected by volume exclusion.

A qualitative comparison of these results with those from the MD simulations of bulk PBD performed by Gee and Boyd¹⁴ and by Kim and Mattice¹⁵ is possible. In the former study, the largest correlation when rotating an α bond is shown to occur between second neighbors for both *cis*- and *trans*-PBD. A detailed analysis of the types of correlated ($i, i \pm 2$) transitions, where i is the rotating bond, is provided therein: these make up 30.1% of all of the α bond transitions in *cis*-PBD and 35.3% in *trans*-PBD. Furthermore, among the coupled transitions between bonds i and $i \pm 2$, 2.6 times as many are reported¹⁴ to occur across the β bond than across the double bond in *cis*-PBD, in qualitative accordance with the present results. This ratio is 0.5 in *trans*-PBD, i.e., correlated transitions most probably occur between α bonds separated by a double bond ($i = 0$ and -2) and not between those separated by a β bond, as in the *cis*

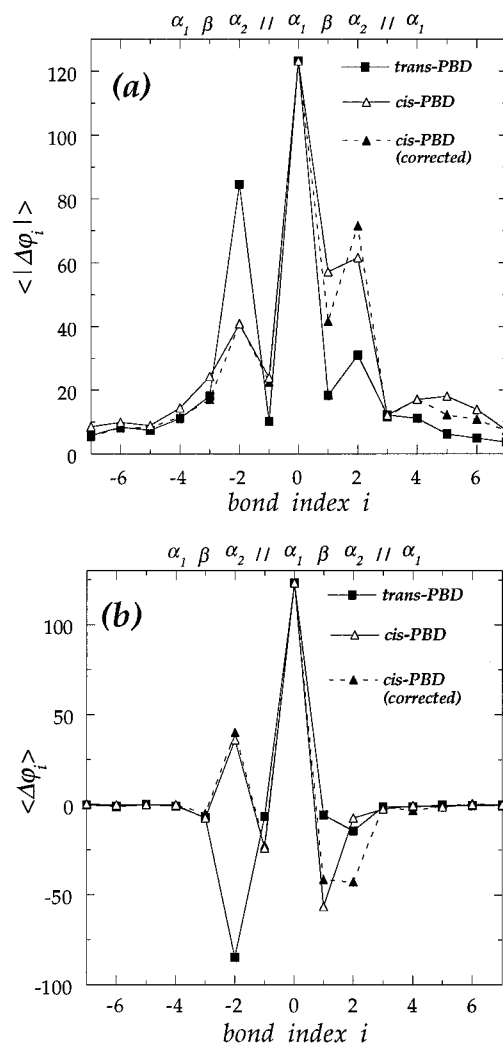


Figure 5. (a) Average absolute changes in the dihedral angles of bonds, $\langle |\Delta\varphi_i| \rangle$, in response to the rotation of α_1 bonds of *cis*- and *trans*-PBD chains with $\xi/\Delta t = 1.62 \times 10^8$ kg/(mol·ns²). The bond labeled as the zeroth undergoes a rotational isomerization. Indexing is performed according to separation from this bond. The types of the rotated bond and its four neighbors on either side are indicated at the top of the figure. Averages are taken over 500 chains with random initial chain configurations in each case. Solid curves are obtained for *cis* and *trans* chains with independent rotameric states assigned to each bond. *cis*-PBD involves strongly disfavored states due to nonbonded interactions; the dashed curve is the corrected result for *cis*-PBD when such configurations are excluded from the generated chains. (b) Average changes in the dihedral angles of bonds, $\langle \Delta\varphi_i \rangle$, in response to the rotation of α_1 bonds of *cis*- and *trans*-PBD chains subject to the same environmental conditions as the chains of (a). Solid curves are obtained for *cis* and *trans* chains with independent bond rotational states. The dashed curve is for the corrected results of *cis*-PBD, obtained with a subset of conformations in which the excluded volume effect is accounted for, as explained in (a).

form. These results are in agreement with the picture provided by CK theory in Figure 5a.

Apart from the absolute changes in dihedral angles, the mechanism of coupling between local torsional motions may be assessed from the $\langle \Delta\varphi_i \rangle$ curves displayed in Figure 5b. Again, the dashed line is obtained by explicitly considering nonbonded interactions. In *trans*-PBD, the rotation of the α bond is accompanied predominantly by a strong (-80°) counterrotation of the second neighbor across the double bond. The other neighbors, which are demonstrated in Figure 5a to undergo some torsional motions in response to the

isomerization of the zeroth bond, do not exhibit a distinct preference for counterrotation or corotation. The situation is different in the *cis* form, where corotations of the α bond across the double bond ($i = -2$) are observed. The first neighboring β bond ($i = 1$) exhibits a counterrotation whose strength is diminished when excluded volume effects are considered. Likewise, the response of the other second neighbor, i.e., the α bond ($i = 2$) next to the β bond on the right, strongly depends on the original set of MC chains considered: a counterrotation is observed only if atoms in the generated chains do not violate their respective van der Waals radii (dashed curve). Neglect of the excluded volume effect leads to an underestimation of the response of that particular bond.

In *trans*-PBD, 67.2% of correlated transitions between second neighbors are reported to occur between the pairs of α bonds flanking the double bond, and 95.8% of them are manifested in the form of counterrotations.¹⁴ That the strongest coupling between bond torsions in *trans*-PBD occurs between the pair of bonds flanking the double bond is unambiguously indicated by the CK results obtained for $i = 0$ and -2 in Figure 5a, and that this coupling is in the form of counterrotations is clear from Figure 5b. Also, the cooperative motion of bonds 0 and 2, i.e., the pair of α bonds flanking a β bond, is reported to involve counterrotations 62.3% of the time, which is also consistent with the present results where a weak tendency to counterrotate is observed in bond $i = 2$. The results concerning the behavior of second neighbors are in agreement with the findings of Kim and Mattice from MD simulations in a similar environment.¹⁵ In the latter study, information is given on the 10 nearest neighbors on either side of the isomerizing bond within 400 ps of rotation in both the *cis* and *trans* forms. The distribution provided by Figure 4 in Kim and Mattice and that of the rotations of the dihedral angles for *trans*-PBD presented in our Figure 5b show close agreement.³⁰

In *cis*-PBD, on the other hand, only 17.9% of all correlated jumps across the double bond are in the form of counterrotations,¹⁴ i.e., the coupling between these α bonds ($i = 0$ and -2) is expressed by corotations, which is in conformity with present predictions. The type of correlation between the pair of α bonds separated by a β bond, on the other hand, is shown in Figure 5a,b of the present work to depend on nonbonded interactions beyond nearest neighbors. Likewise, the coupling between adjacent α and β bonds exhibits some dependence on long-range interactions. MD simulations indicate¹⁴ that 90.9% of the correlated motions between bonds α_1 and α_2 occur in the form of counterrotations. This is mainly due to the excessive occurrence of anticlinic pair inversion across the *trans* conformation of the β bond: $A^+tA^- \leftrightarrow A^-tA^+$ transitions. A preference for counterrotation of the two α bonds is also indicated by the distribution of correlations obtained by Kim and Mattice. Such a preference for counterrotation is obtained in the CK method only if long-range effects are approximately taken into account, as the comparison of the dashed and solid curves at $i = 2$ reveals. At the same time, the preferential response of the first neighbor (β bond, $i = 1$) is weakened. This trend is further enhanced if a subset of MC configurations is considered where the middle repeat unit is constrained to assume the state A^+tA^- in 90% of the MC chains. Also, it will be demonstrated that a slight reduction in the strength of the intermolecular resistance to motion relative to

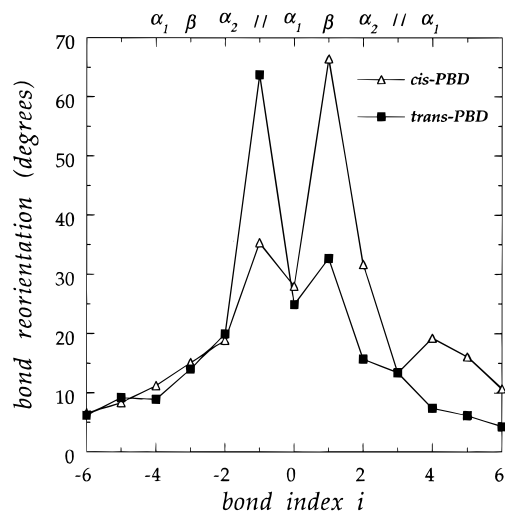


Figure 6. Average spatial reorientations of bond vectors in response to the rotation of α_1 bonds of *cis*- and *trans*-PBD chains, with $\xi/\Delta t = 1.62 \times 10^8$ kg/(mol·ns²). Averaging is performed over 500 chains in each case. Indexing is performed according to separation from a central rotating bond. The types of the rotated bond and the four bonds on either side are indicated at the top of the figure. The results for *cis*-PBD are obtained on the basis of the corrected set of initial configurations from which the dashed curves of Figure 5a,b were drawn.

intramolecular torsional barriers, i.e., decreasing $\xi/\Delta t$, improves the accord between CK predictions and MD simulations.

The preceding comparison of MD simulations and CK predictions provides evidence for the strong effect of long-range intramolecular interactions in *cis*-PBD, which should be explicitly considered for a rigorous assessment of the conformational kinematics. The results for *cis*-PBD in the following are obtained accordingly. It should be noted that the results obtained from CK and MD are in good qualitative agreement in general, although the computational time requirement of the CK approach is 2–3 orders of magnitude lower than that of bulk state MD simulations: the CPU time required by a CK calculation applied to 500 PBD chains with 25 bonds is only 470 s on a Silicon Graphics Challenge L Series computer with 150 MHz R4400 CPU.

We emphasize that the localization mechanisms considered so far occur as a direct consequence of the backbone geometry rather than frictional factors or side group contributions. In fact, Moe and Ediger²⁵ recently performed MD calculations for *cis*-PIP in bulk. According to their calculations, the major response to the isomerization of an α bond is observed at the α bond across the β bond in the form of counterrotations, irrespective of the type of α bond undergoing rotational isomerization. This is in exact agreement with our results. The response of an α bond with a CH₃ group in PIP was observed to be more sluggish, resulting from the enhanced frictional resistance due to the size of this group.

In Figure 6, the average reorientations of bonds in space following the isomerization of an α bond are presented for $\xi/\Delta t = 1.62 \times 10^8$ kg/(mol·ns²). The central bond, which undergoes the torsional rotation, at the same time sweeps an average angular displacement of $\sim 25^\circ$ in space in both the *cis* and *trans* forms. A striking difference in the behavior of *cis* and *trans* chains is observed upon examination of the reorientation of the bonds in the close neighborhood of the zeroth bond: in *trans*-PBD, average reorientations of $\sim 65^\circ$ and

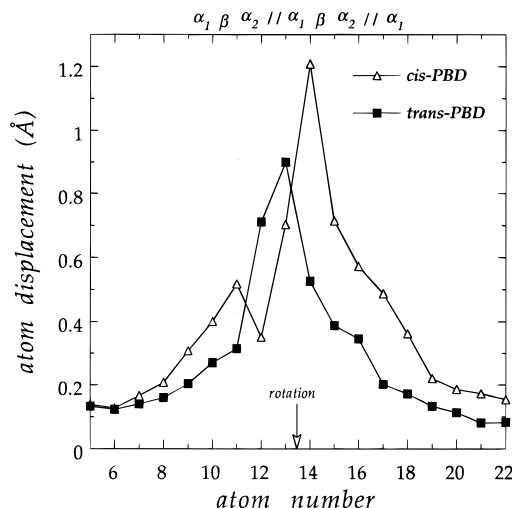


Figure 7. Average spatial displacements of atoms in response to the rotation of α_1 bonds of *cis*- and *trans*-PBD chains, with $\xi/\Delta t = 1.62 \times 10^8$ kg/(mol·ns²). Averaging is performed over 500 chains in each case. The central bond of a chain of 25 bonds, connecting atoms 13 and 14 as indicated on the figure, is rotated by 120°. The types of this bond and its four neighbors on either side are indicated at the top of the figure. The results for *cis*-PBD are obtained by using the corrected set of initial configurations, which lead to the dashed curves of Figures 5a,b.

$\sim 35^\circ$ are undergone by the adjacent double bond ($i = -1$) and β bond ($i = 1$), respectively. The response of the first neighbors is totally reversed in *cis*-PBD. In addition, a considerable amount of reorientation ($\sim 30^\circ$) takes place in the second neighbor across the β bond, as may be observed for the case of $i = 2$. We note that this neighbor is an α_2 bond like the rotating bond itself, which suggests an enhanced cooperativity between the motion of α bonds across the β bond in *cis*-PBD compared to *trans*-PBD.

In Figure 7, the displacements of backbone atoms are compared for *cis*- and *trans*-PBD. Calculations are again obtained from the average of 500 chains in the same frictional environment as before, i.e., $\xi/\Delta t = 1.62 \times 10^8$ kg/(mol·ns²). The atom displacements are in general higher in *cis*-PBD, although the frictional resistance is taken to be the same in both cases. Thus, on the basis of the response of the chain to the isomerization of an α bond, *cis*-PBD exhibits a larger amplitude motion than *trans*-PBD, which is inherently induced by the conformational state of the double bond.

The area under the curves in Figure 7 may be viewed as a measure of the amplitude of local motion undergone by the associated polymer. The areas under the curves for *cis*- and *trans*-PBD are found to be 7.83 and 5.70 Å, respectively. We note that, in Figure 4, which is the counterpart of Figure 7 for the case of a β bond undergoing isomerization, the areas under the curves are 9.19 Å for PE, 11.07 Å for *cis*-PBD, and 11.99 Å for *trans*-PBD. Thus, the rotational transition of an α bond induces a larger scale translation in *cis*-PBD segments, than in *trans*-PBD, whereas that of the β bond results in a slightly more restricted motion in *cis*-PBD. To understand which of the rotations, α or β , plays a predominant role in prescribing the overall conformational kinematics of PBD, we turn to the MD simulations of Gee and Boyd:¹⁴ only 23.6% of all transitions occur at the β bond of *cis*-PBD at 300 K in the bulk state, and the remainder occurs at α bonds. The situation is much more severe for *trans*-PBD, where the percentage of rotating β bonds reduces to 1.8%. These observed percentages are accepted to be proportional to the *a*

priori probabilities of occurrence of the respective transitions. Within the limits of this approximation, the amplitude of local motions in *cis*-PBD appears to exceed that of *trans* chains by a ratio of 1.48:1.00.

Other interesting features that emerge from both Figures 6 and 7 are that, in *cis*-PBD, the most extensive cooperativity during the collective motion of chain segments takes place between units located in the same repeat unit (between two successive double bonds) and that the double bond somehow suppresses the propagation of the motion along the chain. This effect is not distinguishable in *trans*-PBD; on the contrary, the position and orientation of the double bond are observed to be significantly affected by the rotation of the adjoining bond, and, apart from the strong reorientation of the double bond, the translational and orientational motions diffuse almost evenly on both sides of the rotating bond.

Effect of Environment. In the previous CK study,⁹ special attention was given to the effect of environment on chain behavior. It was demonstrated that the type of coupling between bond torsions depends on the interplay between intramolecular effects and environmental friction, accounted for through the ratio given by eq 6. The precise values of the ratio corresponding to the bulk state simulations mentioned earlier are not known. It is of interest to find out whether changes in the frictional resistance of the surrounding medium would induce modifications in the mechanisms of various relaxation phenomena.

An examination of eq 6 reveals that changing k_0 is equivalent to a proportional change in the strength of internal barriers to rotation relative to frictional effects. In this section, we concentrate on the α bonds whose transition probabilities are higher due to the low barrier heights between rotameric states, as previously discussed. We further restrict the analysis to *cis*-PBD, which is experimentally and commercially more important. In fact, negligible differences are observed in the localizing motions of *trans*-PBD; the governing mechanisms remain unaltered to changes in the environmental conditions in response to the isomerization of α bonds.

In the following, the $\xi/\Delta t$ value is varied by a factor of 20 between 1.62×10^7 and 3.24×10^8 kg/(mol·ns²). Excluded volume effects are considered when generating the original chains in all cases. In Figure 8a, the absolute changes in the dihedral angles, $\langle |\Delta\varphi_i| \rangle$, of *cis*-PBD upon the manipulation of $\xi/\Delta t$ values are presented for the rotational isomerization of α_1 bonds. The corresponding $\langle \Delta\varphi_i \rangle$ curves are given in Figure 8b. An increase in $\xi/\Delta t$ is equivalent to increasing the strength of the frictional resistance relative to intramolecular torsional potentials. Alternatively, this may be viewed as diminishing the intramolecular barriers to rotation in a given environment and gradually approaching the behavior of a freely rotating chain of equilibrium statistics, where internal rotational barriers have little importance and the dynamics is controlled by the surrounding medium. An examination of Figure 8a,b shows that the mechanism of conformational relaxation is not affected by the frictional effects, in general. By adopting $\xi/\Delta t \approx 2 \times 10^7$ kg/(mol·ns²), the behavior predicted by the MD simulations in the bulk state is obtained, i.e., the second neighboring α bond across the β bond undergoes the largest torsion in response to the rotation of an α bond.

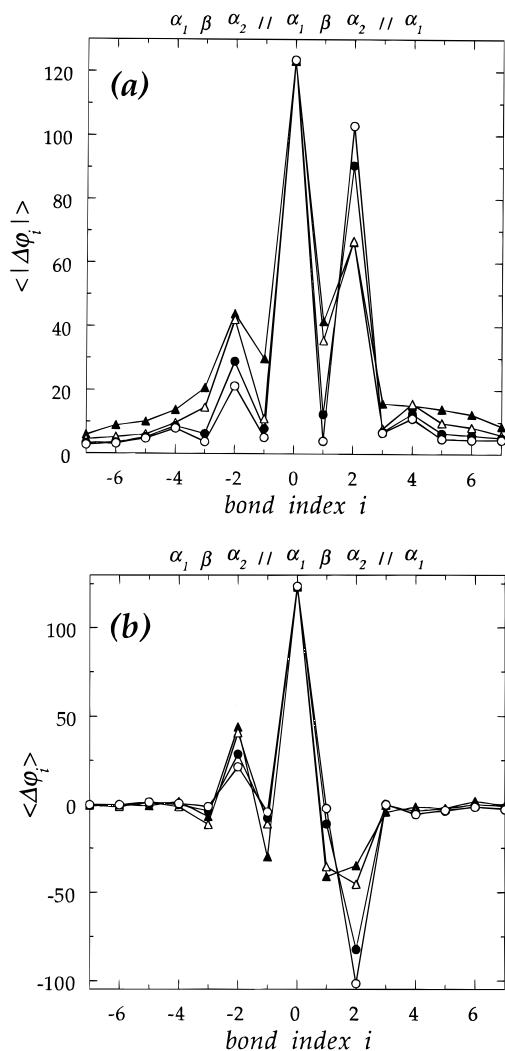


Figure 8. (a) Effect of changing environmental conditions on average changes in dihedral angles, $\langle \Delta\varphi_i \rangle$, of cis -PBD in response to 120° rotation of α_1 bonds. Results are displayed for the following $\xi/\Delta t$ values: 1.62×10^7 (○), 2.16×10^7 (●), 3.24×10^7 (△), and 32.4×10^7 kg/(mol·ns²) (▲). (b) Effect of increasing friction coefficient on average changes in the dihedral angles of bonds, $\langle \Delta\varphi_i \rangle$, of cis -PBD in response to 120° rotation of α_1 bonds. $\xi/\Delta t$ values are the same as those in (a). As the friction coefficient is lowered, i.e., the role of intramolecular torsional potentials is emphasized, the counterrotations induced at the α bond across the β bond ($i = 2$) become more pronounced, whereas those occurring at the β bond are almost eliminated.

The effect of a changing environment on the reorientation of bond vectors is displayed in Figure 9. The $\xi/\Delta t$ values considered are in the same range as those of Figure 8a,b. Excluded volume effects are taken into consideration in each case. The rotameric transition occurs at bond 0. Increasing the friction coefficient tends to decrease the reorientation of the neighboring β bond ($i = 1$), while the reorientation of the first neighboring double bond ($i = -1$) and that of the nearest α bonds on both sides ($i = \pm 2$) increase.

Another interesting feature that emerges in PBD chains irrespective of the type of conformer ($cis/trans$) or the type of bond going through rotameric transition (α/β) is that the reorientations and atomic displacements of the farther neighbors ($|i| \geq 6$) do not depend on the environmental friction. In the previous CK study⁹ where the corresponding displacements of PE chains were investigated, some dependence of these localization mechanisms on the friction coefficient was observed.

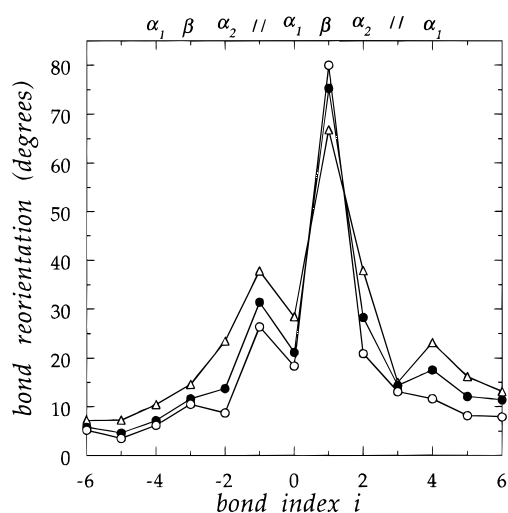


Figure 9. Reorientation of bond vectors in response to bond isomerization in various frictional environments for cis -PBD. The rotated bond is of type α_1 in the middle of 25 bond chains and is labeled as the zeroth. Averaging is performed over 500 chains where van der Waals interactions are taken into account in the initial structures. $\xi/\Delta t$ values and the corresponding symbols are 1.62×10^7 (○), 2.16×10^7 (●), and 3.24×10^7 kg/(mol·ns²) (△). The reorientation of the bonds beyond sixth neighbors on both sides are the same, irrespective of the friction coefficient considered.

This invariance in PBD chains is attributed to the constraints induced by the existence of rigid double bonds.

Concluding Remarks

In this study, the effect of chain geometry on the kinematics of local motions is investigated by comparing the behavior of cis - and $trans$ -PBD and that of the previously studied PE chains. The fact that chains possessing backbone geometry different from that of PE may exhibit distinct relaxational mechanisms was first pointed out by Adolf and Ediger in their BD study comparing the local dynamics of PE and PIP chains.²⁴ It was stated therein that second neighbor coupling in PE was different from that in PIP and that torsional coupling decreased with separation along the chain. The present study complements their work by showing the importance of the type of the bond on relaxational mechanisms in cis - and $trans$ -PBD. Our observations may be summarized as follows: (i) An α bond isomerization most frequently induces a rotational motion in the nearest α bond, as shown in Figure 5. (ii) Upon rotation of an α bond, the strongest orientational and translational coupling is observed in the first neighboring β bonds in cis -PBD and in the first neighboring double bonds in $trans$ -PBD, as may be seen in Figures 6 and 7. (iii) The isomerization of an α bond in $trans$ -PBD is systematically accommodated by the counterrotation of the α bond across the double bond. In cis -PBD, the same two α bonds exhibit corotations. (iv) Furthermore, in cis -PBD, major coupled torsions in the form of counterrotations take place at the second neighboring α bond across the β bond. (v) The isomerization of β bonds is distinguished by the strong correlations extending up to third and fourth neighboring bonds along the chain. (vi) Nonbonded intramolecular interactions have a strong influence on conformational relaxation in cis -PBD. This influence is negligibly small in $trans$ -PBD. (vii) Under the same frictional environmental conditions, cis -PBD exhibits a larger amplitude

motion in response to bond isomerization than *trans*-PBD by a factor of ~ 1.5 . (viii) Coordinated translational motions of atoms are observed in *cis*-PBD within the repeat unit where isomerization occurs. In *trans*-PBD, on the other hand, only the position and orientation of the neighboring double bond are significantly affected (Figures 6 and 7). (ix) The mechanism of motion is predominantly sensitive to backbone geometry and energetics, but is relatively insensitive to frictional resistance, as demonstrated in Figures 8a,b and 9. This is also confirmed by the MD simulations of PIP in the bulk state.²⁵

In the CK method, bond lengths and bond angles are constrained to fixed values. The use of holonomic constraints for bond lengths is justifiable on the basis of the stiffness of the harmonic potentials governing bond stretching. The distortion of bond angles, however, may contribute to the mechanism of relaxation. The CK formalism may be easily extended to include the effect of bond bending potentials, if the kinematics of polymers with soft bond angles, such as siloxanes, is explored. In the present case, however, the neglect of this degree of freedom seems to be inconsequential. Besides, small amplitude torsional motions within the rotational energy wells, which are more important than bond angle distortions, are rigorously accounted for in the CK approach. In fact, CK gives information on the fluctuations in torsional angles, i.e., on the amplitudes of the cooperative librational motions at rotational minima, which do not necessarily result in isomerization, but play an important role in the localization of a motion.

Finally, it is worth pointing out that the CK method is computationally very efficient compared to other simulation techniques. Detailed results that show close agreement with MD and BD simulations are presently obtained within time scales at least 2 orders of magnitude lower.

Acknowledgment. Partial support from Bogazici University Research Funds Project No. 95P0056 is gratefully acknowledged.

References and Notes

- (1) Helfand, E. *J. Chem. Phys.* **1971**, *54*, 4651.
- (2) Weber, T. A.; Helfand, E. *J. Phys. Chem.* **1983**, *87*, 2881.
- (3) Monnerie, L. *Gazz. Chim. Ital.* **1987**, *117*, 139.
- (4) Adolf, D. B.; Ediger, M. D. *Macromolecules* **1991**, *24*, 5834.
- (5) Ediger, M. D.; Adolf, D. B. *Adv. Polym. Sci.* **1994**, *116*, 73.
- (6) Bahar, I.; Erman, B.; Monnerie, L. *Adv. Polym. Sci.* **1994**, *116*, 145.
- (7) Helfand, E.; Wasserman, Z. R.; Weber, T. A. *Macromolecules* **1980**, *13*, 526.
- (8) Haliloglu, T.; Bahar, I.; Erman, B. *J. Chem. Phys.* **1992**, *97*, 4428.
- (9) Baysal, C.; Erman, B.; Bahar, I. *Macromolecules* **1994**, *27*, 3650.
- (10) Rigby, D.; Roe, R. J. *J. Chem. Phys.* **1989**, *22*, 2259.
- (11) Takeuchi, H.; Roe, R. J. *J. Chem. Phys.* **1991**, *94*, 7446.
- (12) Zuniga, I.; Bahar, I.; Dodge, R.; Mattice, W. L. *J. Chem. Phys.* **1991**, *95*, 5348.
- (13) Boyd, R. H.; Gee, R. H.; Han, J.; Jin, Y. *J. Chem. Phys.* **1994**, *101*, 788.
- (14) Gee, R. H.; Boyd, R. H. *J. Chem. Phys.* **1994**, *101*, 8028.
- (15) Kim, E.-G.; Mattice, W. L. *J. Chem. Phys.* **1994**, *101*, 6242.
- (16) Glauber, R. J. *J. Math. Phys.* **1963**, *4*, 294.
- (17) Orwoll, R. A.; Stockmayer, W. H. *Adv. Chem. Phys.* **1969**, *15*, 305.
- (18) Moro, G.; Nordio, P. L. *Mol. Phys.* **1985**, *56*, 255.
- (19) Moro, G.; Nordio, P. L. *Mol. Phys.* **1986**, *57*, 947.
- (20) Bahar, I.; Erman, B. *Macromolecules* **1987**, *20*, 1369.
- (21) Bahar, I.; Erman, B.; Monnerie, L. *Macromolecules* **1992**, *25*, 6309.
- (22) Bahar, I.; Erman, B.; Monnerie, L. *Macromolecules* **1992**, *25*, 6315.
- (23) Bahar, I.; Baysal, N.; Erman, B.; Monnerie, L. *Macromolecules* **1995**, *28*, 1038.
- (24) Adolf, D. B.; Ediger, M. D. *Macromolecules* **1992**, *25*, 1074.
- (25) Moe, N. E.; Ediger, M. D. *Polymer*, submitted.
- (26) Rey, A.; Kolinski, A.; Skolnick, J. *J. Chem. Phys.* **1992**, *97*, 1240.
- (27) Abe, Y.; Flory, P. J. *Macromolecules* **1971**, *4*, 219.
- (28) Li, Y.; Mattice, W. L. *Macromolecules* **1992**, *25*, 4942.
- (29) Kim, E.-G.; Misra, S.; Mattice, W. L. *Macromolecules* **1993**, *26*, 3424.
- (30) In comparing the two pictures, we note that the bond subject to full rotation in their study is α_2 , in contrast to the α_1 bond rotated here. For this reason, the two figures are mirror images of each other with respect to the $i = 0$ axis.

MA950847T